Reduction of harmonics emission of a WECS in the electrical grid using multilevel inverters

Maha annoukoubi[1], Ahmed essadki[1], Hammadi laghridat[1], Tamou nasser[2]
[1]National School of Arts and Crafts in Rabat (ENSAM), Mohammed V University, Rabat, Morocco
[2]National High School for Computer Science and Systems Analysis (ENSIAS), Mohammed V University, Rabat, Morocco

## Article Info

ABSTRACT

Wind energy conversion system (WECS) is composed of many non-linear power electronic sub systems, which contribute significantly in harmonic emissions that is a threat for the quality of electrical power. Hence, for a better integration of WECS in the electrical grid and in order to satisfy IEEE 519 standards, WECS must inject a quality power with a rate of total harmonics distortion (THD) that is less than 5%. Multilevel Inverters are an emerging solution for having a perfect sinusoidal output voltage with minimum harmonic content and lower switching losses than the two-level inverter so that only a smaller filter size is required. Thus, in this paper we are presenting a significantly improved results of the reduction of the grid injected current THD using three types of inverters (two-levels, three-levels NPC, and five-levels H-bridge cascade) for a WECS and comparing the THD performances of using each of the studied inverter. All results of THD are verified by a Fast Fourier transform simulation using MATLAB/Simulink.
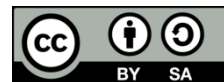
Corresponding Author:

Maha Annoukoubi
Research Center for Engineering and Health Sciences and Technologies,
National School of Arts and Crafts in Rabat (ENSAM), Mohammed V University, Morocco
Email: m.annoukoubi@gmail.com

1. INTRODUCTION

In the last few decades, our World has known a remarkable rise of the annual rate of population and urbanization which is estimated to 1.2%. As result, the rate of energy demand especially domestic electrical energy has grown up consequently over the 2009-2019 period to reach 23 430 TWh in 2019. In 2020, the world experienced a new tragic pandemic COVID-19 which turned our daily lives into disorder but despite all of that, this pandemic had a positive impact in the global primary energy consumption which fell by 4.5% that was considered as the largest decline since 1945. Also, the domestic electrical demand was declined for the first time since 2009 by 1.1% to reach 23 176 TWh as shown in Figure 1, according to enerdata statistics and statistical review of world energy 2021 [1], [2].

The global carbon emission from energy use was also estimated to have fallen by 6.3% since 2011 as a positive result of the pandemic [2]. Staring from what's happened last year, knowing the importance of reducing energy demand especially the non-renewable energy because of their negative environmental impact and the fact they are in limited supply. Also, since 2015 in the Paris Conference of Parties (COP21) there has been a huge interest and ambitions to decarbonize by most of countries which lead them to carry investigation in order to minimize the use of fossils fuels in electrical energy production and maximize the contribution of renewable energies such Wind, solar, geothermal. So, despite the disorder of 2020, renewable energy, continued to have a remarkably growth, wind and solar capacity increased by 238 GW last year

which is 50% higher than other last years. In the same way, the share of wind (173 TWh) and solar (148 TWh) generation in the global power mix have known the biggest increase ever. Other way to increase and ameliorate the participation of Renewable energy in responding to the global electrical energy demand is encouraging each country to do its role. Indeed, in response to that our country Morocco decide to exceed objectives announced at COP21 by increasing the share of energies to more than 52% in the electricity mix by 2030 for that we have 50 renewable projects with a total installed capacity of around 4 GW that are already in operation. Morocco has more than 40 international companies that are active in a renewable power generation market. Since 2009, more than 12 billion dollars are invested in renewable energy. These projects have contributed to improve our energy independence by more than 8% since 2009, other projects are being developed or under construction and the multiple others will be financed over the next decade. In the same way Morocco encourage researchers to do research and studies in this fields thing that going to be subject of our article.
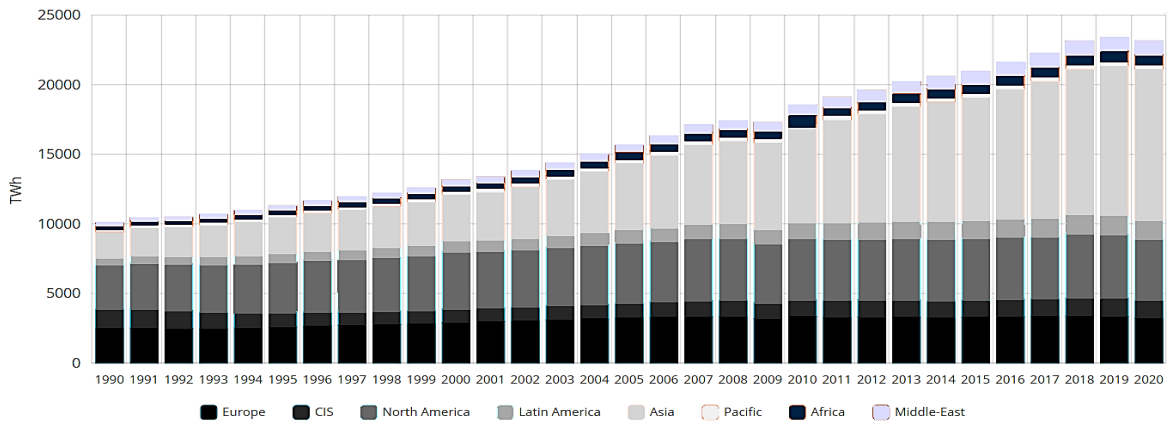

Figure 1. Electrical energy demand over 1990-2020 (TWh) [1]

Wind is considered as one of the most renewable sources of energy. It is used to generate electricity from kinetic energy created by reason of the air motion; this generation is taking place using an electrical system called wind energy conversion system which transforms the wind energy into mechanical energy and then to an electrical one and that through many electrical and mechanical sub-systems that will be more developed in this article. The electrical energy generated by wind systems has known an enormous growth over the last years and its penetration into the power system have increased consequently so according to wind power statistics of the World Wind Energy Association, the installed wind capacity has reached 744 GW by end of 2020 [2]. The Figure 2 shows the worldwide evolution of the total cumulative installed capacity through the 6 last years.
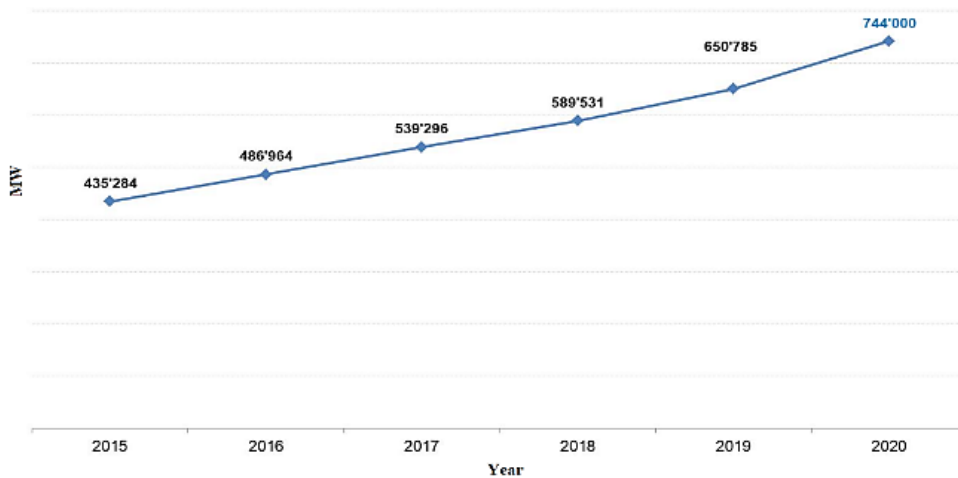

Figure 2. Total cumulative installed capacity over 2015-2020 [2]

To generate electricity from wind we have to pass by four essential sub-systems, described at Figure 3, so at first the wind hits the turbine's blades and makes it rotate around a rotor that is connected to a gearbox which multiple the number of tours to an adaptive one and transmit it to the generator through the drive shaft, this generator converts the mechanical power into an electrical one that is injected to the grid through power converter. The combination of all these elements forms the wind energy conversion system (WECS) [3]. The total cumulative f power produced by the systems can vary depending on the size of the turbine and the length of its blades. The output depends on the rotor dimensions and the cube of the wind speed. So automatically, when wind speed increase, wind power generated increases.
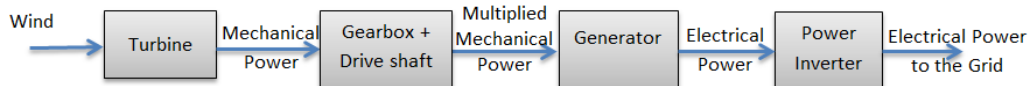

Figure 3. WECS blocs

Since the power inverter plays a vital role in the WECS by connecting the power generator to the electrical grid in order to inject the electrical power generated and by converting DC power to AC and AC to DC to be suitable for the bidirectional power flow; There have been many developments and ameliorations in power electronic converters [4]. These converters are commonly used to regulate and adapted the electrical signal to the required form and parameters for a better integration in the grid and that's by respecting the IEEE conditions for grid integration which consist on limiting of the total harmonic distortion (THD) in less the 5%. Indeed, power inverters become subject of several work and studies in order to attain the best topology which would make the penetration of the generated power easier and better.

In 1980's, as result of researchers' investigations they have developed a new configuration of inverters called Multilevel inverter [5], [6]. A multi-level inverter is a power electronic system which provides an output alternating voltage level by using a number of DC voltage in input depending on the number of levels that will be obtained. The notion of multi-level inverter is a change made on the conventional two level one which gives an output wave form that varies between two values. So, the aim of multi-level inverter is to generate a smoother output waveform depends on the level, more level means that the output voltage will be smoother and near to a sinusoidal output. Multilevel inverters are very promising because of the many advantages they present as having a current with a reduced THD factor, lower stress of the electronic components due to decreased voltages, switching losses that are lower than those of conventional two-level inverter and also a smaller filter size is required, and lower electromagnetic interference (EMI), all of that make the multilevel inverter low-priced than the conventional one [7].

The purpose of this article is to present a comparative study and analyze of 3 different multilevel topologies of inverter that will be used in our wind energy conversion system and that's in a way to prove that the current's THD will be reduced by increasing the level of the multilevel inverter for a better integration in the grid also by improving and smoothing the output voltage waveform. Also, for a better penetration of the grid a control methodology of active and reactive power is proposed. The current paper is organized as follows. The introduction is presented in the first section. The section 2 presents a modeling of all WECS subsystems. Then, the analyze and model of two-level, three-level and five-level inverters are given in the section 3. After that we present in section 4 the control strategy used in our WECS. In the section 5 simulations results in MATLAB/Simulink are presented and discussed. Last section concludes about the results obtained and gives an overall view of our further works.

2. DYNAMIC MODELING OF WIND TURBINE SYSTEM USING A DFIG

The aim of a wind energy conversion system is transforming wind kinetic energy into an electrical one. WECS is composed generally of a wind turbine transforming the wind energy into a mechanical one, a gearbox which adapts the rotation speed, a generator that transforms the mechanical power to an electrical one and power electronics in order to inject the generated power directly to the grid. In this section, we are presenting the model of each part of this system as in [8]. First, we are modeling the aerodynamic wind turbine that is composed of a horizontal three-blade and blades rotor which is linked to the gearbox using a low-speed shaft. Then we will present the model of the used generator which is a doubly fed asynchronous generator (DFIG) that we have selected for the many advantages it presents comparing to other generators. This one is directly connected to the grid using two power multilevel converters and for a better integration the use of controller is essential in our system; we are using the PI Controllers in both rotor side and grid side with

MPPT controller for a maximum power extraction and a pitch control. Our WECS is described in Figure 4 and power system data is summarized in the Table 1. Table 1 shows the parameters of our wind energy conversion system.
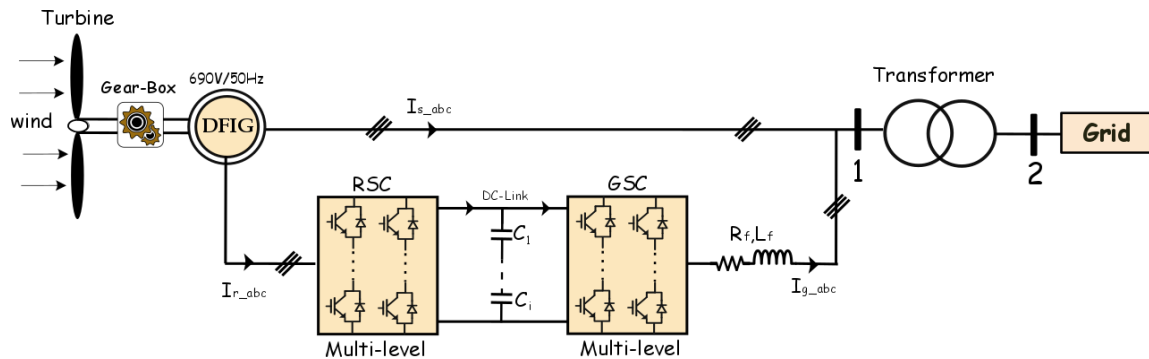

Figure 4. Global scheme of WECS connected to the grid

Table 1. Turbine, DFIG, and grid side parameters

Parameters	Values	Parameters	Values
Rated power	1.5 MW	Stator Resistance R_s	2.65 mΩ
Rated wind speed	12 m/s	Rotor Resistance R_r	2.63 mΩ
Density of Air	1.225 kg/m³	Stator Leakage Inductance $L_{s\sigma}$	0.1687 mH
Blade radius	31 m	Rotor Leakage Inductance $L_{r\sigma}$	0.1337 mH
Gearbox ratio G	59	Magnetizing Inductance L_m	5.4749 mH
Rated Power Pn	1.5 MW	DC-Link Voltage V_{dc}	1320 V
Rated Voltage Un	690 V	DC-Link Capacitor C	10028.7 μF
Nominal Frequency	50 Hz	Filter Resistance R_f	0.1838 Ω
Rated Rotor Speed	1750 tr/min	Filter Inductance L_f	0.61187 mH
Number of Pole Pairs	2		

2.1. Wind turbine dynamic modeling

The aerodynamic model of the wind turbine system has been studied and presented in several works [9], [10]. This part aims to transform the incoming air into a mechanical power using the aerodynamic equation below and to transmit it to the generator through the gearbox, the Figure 5 present the 3D characteristic of aerodynamic power:

$$P_{aero} = C_p(\lambda, \beta)P_w = C_p(\lambda, \beta) \frac{1}{2} \rho A_{wt} w_t^3 \qquad (1)$$

P_w is the wind's kinetic power; C_p is the power coefficient depending on the blades pitch angle β and the turbine tip speed ratio λ; A_{wt}, ρ and w_t are the turbine blades area, the air density and the wind speed.

The tip speed ratio is given by (2):

$$\lambda = \frac{R \, \Omega_{tur\_i}}{w_{t\_i}} \qquad (2)$$

Ω_{tur_i} is the speed of turbine, and R is the radius of turbine blades.

Mechanical angular speed ω_{mec} and Gearbox torque T_g are expressed as follow, where G is the gearbox coefficient.

$$T_g = \frac{T_{aero}}{G} \qquad (3)$$

$$\omega_{mec} = G \, \omega_{tur} \qquad (4)$$

The mechanical equation of our system is:

$$J \frac{d\omega_{mec}}{dt} = T_g - T_{em} - f \, \omega_{mec} \qquad (5)$$

T_{em} and f are the DFIG electromagnetic torque and the friction coefficient. J represents the total inertia that can be expressed as (6):

$$J = \frac{J_{tur}}{G^2} + J_{DFIG} \tag{6}$$

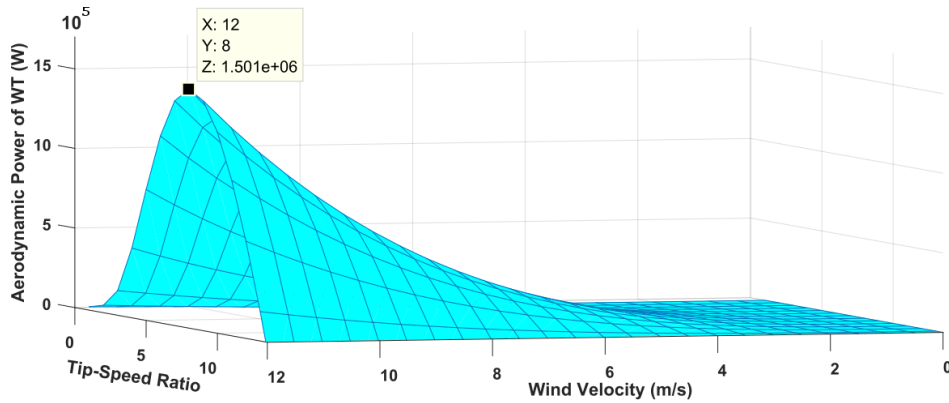J_{DFIG}, J_{tur} are the inertias of the generator and the turbine.

Figure 5. 3D characteristic of aerodynamic power

2.2. DFIG dynamic model

To convert the mechanical power Pm produced by the turbine to an electrical power, a generator system is required. Several types of generators exists but for this work we are using the doubly fed induction generator DFIG because it is the most used system for variable speed WECS as studied in [11]–[14]. In this part, we are presenting DFIG equations in park reference *dq* linked to a rotating field. For simplifying those equations, we use a Park reference linked to the rotating field and the hypothesis of a stator flux is constant and oriented along the axis d and stator resistance as negligible. The stator and rotor generator *dq* equivalent model is presented in Figure 6.
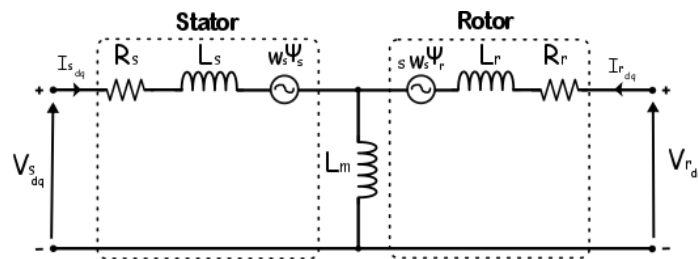

Figure 6. DFIG equivalent model in *dq*

The DFIG model is represented by the following equations:

$$\begin{bmatrix} v_{sd} \\ v_{sq} \\ v_{rd} \\ v_{rq} \end{bmatrix} = - \begin{bmatrix} R_s & 0 & 0 & 0 \\ 0 & R_s & 0 & 0 \\ 0 & 0 & R_r & 0 \\ 0 & 0 & 0 & R_r \end{bmatrix} \begin{bmatrix} i_{sd} \\ i_{sq} \\ i_{rd} \\ i_{rq} \end{bmatrix} + \frac{d}{dt} \begin{bmatrix} \Psi_{sd} \\ \Psi_{sq} \\ \Psi_{rd} \\ \Psi_{rq} \end{bmatrix} + \begin{bmatrix} 0 & -\omega_s & 0 & 0 \\ \omega_s & 0 & 0 & 0 \\ 0 & 0 & 0 & -s\omega_s \\ 0 & 0 & s\omega_s & 0 \end{bmatrix} \begin{bmatrix} \Psi_{sd} \\ \Psi_{sq} \\ \Psi_{rd} \\ \Psi_{rq} \end{bmatrix} \tag{7}$$

i, v and Ψ are the current, the voltage and the DFIG field. L and R are the inductance and the resistance; s and r indicate the side stator and the side rotor of generator and ω_s is the electrical angular speed of the DFIG. Stator and rotor magnetic fields equation are:

$$\begin{bmatrix} \Psi_{sd} \\ \Psi_{sq} \\ \Psi_{rd} \\ \Psi_{rq} \end{bmatrix} = \begin{bmatrix} -L_s & 0 & L_m & 0 \\ 0 & -L_s & 0 & L_m \\ L_m & 0 & -L_r & 0 \\ 0 & L_m & 0 & -L_r \end{bmatrix} \begin{bmatrix} i_{sd} \\ i_{sq} \\ i_{rd} \\ i_{rq} \end{bmatrix} \tag{8}$$

L_s; L_r and L_m are the stator inductance; the rotor inductance and the mutual inductance. Equations of electrical active and reactive powers delivered by the DFIG are expressed as:

$$\begin{bmatrix} P_s \\ Q_s \end{bmatrix} = \frac{3}{2} \begin{bmatrix} v_{sd} & v_{sq} \\ v_{sq} & -v_{sd} \end{bmatrix} \begin{bmatrix} i_{sd} \\ i_{sq} \end{bmatrix} \tag{9}$$

$$\begin{bmatrix} P_r \\ Q_r \end{bmatrix} = \frac{3}{2} \begin{bmatrix} v_{rd} & v_{rq} \\ v_{rq} & -v_{rd} \end{bmatrix} \begin{bmatrix} i_{rd} \\ i_{rq} \end{bmatrix} \tag{10}$$

2.3. Mode of the grid side RL filter

WECS inject the generated power to the grid through an RL filter, the model of this filter is expressed as follow:

$$\begin{bmatrix} v_{gd} \\ v_{gq} \end{bmatrix} = \begin{bmatrix} -L_f & 0 \\ 0 & -L_f \end{bmatrix} \frac{d}{dt} \begin{bmatrix} i_{gd} \\ i_{gq} \end{bmatrix} + \begin{bmatrix} -R_f & \omega_e L_f \\ -\omega_e L_f & -R_f \end{bmatrix} \begin{bmatrix} i_{gd} \\ i_{gq} \end{bmatrix} + \begin{bmatrix} v_{id} \\ v_{iq} \end{bmatrix} \tag{11}$$

where v_{fd} and v_{fq} are the output voltage of the filter in d-q ; i_{fd} and i_{fq} are the filter current; the voltages v_{id} and v_{iq} are inverter's output voltage in d-q frame; R_f and L_f are the resistance and the inductance of the filter.
The resulted active and reactive powers (P_{wt} ,Q_{wt}) that will be injected to the grid are expressed by:

$$\begin{bmatrix} P_{wt} \\ Q_{wt} \end{bmatrix} = \begin{bmatrix} P_s \\ Q_s \end{bmatrix} + \begin{bmatrix} P_g \\ Q_g \end{bmatrix} \tag{12}$$

3. MODEL OF MULTILEVEL INVERTERS AND THEIR IMPACT IN TERMS OF HARMONICS

Recently, multilevel inverters have known an important development especially in terms of grid's connection with WECS. A multilevel inverter is a power electronic system that enables obtaining a specific alternative output voltage from a DC input voltage; it is a new concept that brings new modification and amelioration to the conventional two-level inverter. The aim of multi-level inverter is to generate a smoother output waveform depends on the level, more level means that the output voltage will be smoother and near to a sinusoidal output. Multilevel inverters are very promising because of the many advantages presented at [15], [16] in terms of improving power quality and higher voltage capability; providing a current with a reduced THD factor; low THD; lower stress of the electronic components due to decreased voltages; switching losses that are lower than those of conventional two-level inverter; smaller filter size is required; lower EMI; and low-priced than the conventional one.

3.1. Multilevel topologies

Various topologies for multilevel inverters have been proposed since the development and improvement of the power semiconductors as the insulated gate bipolar transistor (IGBT) and metal oxide semiconductor field effect transistor (MOSFET); Common ones are diode clamped, flying capacitor or multi-cell, cascaded H-bridge, and modified H-bridge multilevel and they are all differentiated by their topologies and control methods as presented in Figure 7 [17]:

− The neutral point clamped (NPC) inverter which was the first multilevel topology that was proposed by Nabae [5]. They are using clamping diodes for guaranteeing the proper voltage sharing across the power switches and as result, it decreased the THD factor in output voltage and current and smooth their waveforms. Despite the advantage of this topology but it is limited only in three levels and that due to the arrangement complexity of power semiconductors in higher levels.
− Flying capacitor is a developed topology of NPC that replaced the use of diode by capacitor [18]. This structure gives more flexibility in waveform synthesis and balancing voltage. Redundancy in the switching states is available by using flying capacitors instead of clamping diodes. And it could be utilized to control the regulation of the capacitor voltages.

− H-bridge structures [19], [20], which has known a high interest due to the greater demand of medium-voltage high power inverters. The H-bridge cascaded inverter uses series of single-phase full-bridge inverters to construct multilevel phase legs wit separate dc sources.
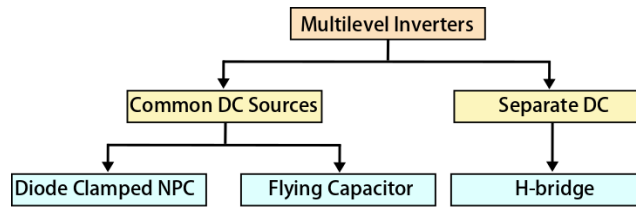

Figure 7. Multilevel inverters topologies

3.2. Harmonic impact

Harmonic emissions are identified as a main power quality problem for WECS, that's why it is essential to understand harmonic behavior of WECS in order to control their effect on the electrical grids to assure a good connection. In the power system, the definition of a harmonic can be stated as follows: a periodic sinusoidal component having a frequency integer multiple of the frequency of the fundamental [21]. So, for a system, the fundamental frequency is f_0 and the harmonic h^{nd} frequency is hf_0. Harmonics are often used to define the distortion of the sinusoidal signal associated with current or voltage of different amplitudes and frequencies which results a degradation of the power factor.

The concept of harmonic was introduced at the beginning of the 19th century by Joseph Fourier who demonstrated that any periodic non-sinusoidal signal can be represented by a sum or series of sinusoids of discrete frequencies, multiple.

$$f(t) = \frac{a_0}{2} + \sum_{n=1}^{\infty}\big(a_n\cos(n\omega t) + b_n\sin(n\omega t)\big) \tag{13}$$

where a_0, a_n and b_n are defined as:

$$a_0 = \frac{1}{2\pi}\int_0^2 f(\omega t)d(\omega t) \tag{14}$$

$$a_n = \frac{1}{\pi}\int_0^{2\pi} f(\omega t)\cos(n\omega t)d(\omega t) \tag{15}$$

$$b_n = \frac{1}{\pi}\int_0^2 f(\omega t)\sin(n\omega t)d(\omega t) \tag{16}$$

The first component of rank 1 (h = 1) is called: fundamental component. For systems connected to a stabilized electrical grid, the frequency of the fundamental component is considered as fixed, 50 Hz in Europe and 60 Hz in the United States. The rest of the components of the series FOURIER are called: harmonics of order h, where h designates the number of the component, order 2 corresponds to the second term of the FOURIER series which will have a frequency double of the fundamental. Figure 8 gives an example of a current containing a third harmonic, i.e., a current which contains a rank 3 component high in amplitude. In three-phase electrical grid, the main harmonic components are of ranks 5, 7, 11 and 13.
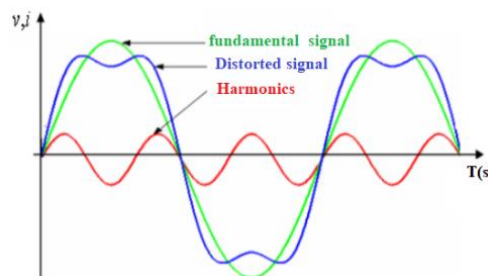

Figure 8. Representation of the effect of a harmonic

The presence of current or voltage harmonics leads to negative effects on the distribution grid as studied in [22], such as:

− Heating of conductors, cables, capacitors and machines due to additional copper and iron losses.
− Electronic equipment may be sensitive to the voltage distortion supplying it, due to higher voltage peaks, unexpected zero-crossing, and affectation to protection circuits.
− Reduced service life of components and equipment under continuous distorted supply voltage.
− Resonance phenomena. The resonant frequencies of the circuits formed by the transformer inductors and the capacitances of the cables are normally quite high, but these can coincide with the frequency of a harmonic. In this case, there will be a significant amplification which can destroy the equipment connected to the grid.
− Interference induced on communication lines, particularly electromagnetic radiation.

3.3. Total harmonic distortion

It is defined as a ratio between the r.m.s. value of all the harmonics and the r.m.s. of the fundamental frequency. It is usually given as a percentage [%] (by multiplying previous result per 100) [23]. Current THD: according to the definition above, the THD for current will be,

$$THD_i = \sqrt{\sum_{n=2}^{N}\left(\frac{I_n}{I_1}\right)^2} \tag{17}$$

Voltage THD (THDv): similarly, the THD of voltage is expressed as,

$$THD_v = \sqrt{\sum_{n=2}^{N}\left(\frac{v_n}{U_1}\right)^2} \tag{18}$$

In order to respect the IEEE conditions for grid integration which consist on limiting of the THD in less than 5%. The use of multilevel inverters seems to be a good solution to produce a stepped output phase voltage with a refined harmonic profile compared to a two-level inverter.

3.4. Model of the two-level inverter

A two-level inverter is a DC/AC converter that produces two different output voltages + Vdc/2 and – Vdc/2 from an input voltage Vdc and in order to create an AC voltage, these two generated voltages are continually switched. For switching we used a pulse width modulation (PWM). This method of generating AC output from a DC one can be effective but it has few drawbacks in creating harmonic distortions in the output voltage, it also has a high dv/dt comparing to the one providing by the multilevel inverter [24]. For this work we are using a three-phase two-level inverter that is composed of 3 arms each one consists of two switches controlled using a PWM Signal presented in the Figure 9.
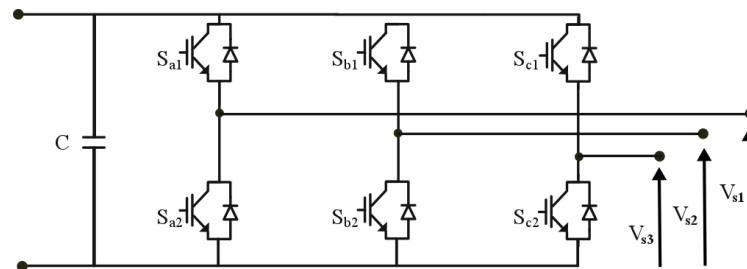

Figure 9. Configuration of a two-level inverter

The two-level converter function matrix is presented as:

$$\begin{bmatrix}V_{s1}\\V_{s2}\\V_{s3}\end{bmatrix} = \frac{2}{3}U_c\begin{bmatrix}1 & -1 & -1\\-1 & 1 & -1\\-1 & -1 & 1\end{bmatrix}\begin{bmatrix}S_a\\S_b\\S_c\end{bmatrix} \tag{19}$$

In MATLAB/Simulink we modeled and simulated the two-level inverter as a part from the WECS in order to observe the output waveform and analyze the THD before using it with WECS. Figure 10(a)

present a single-phase two-level output voltage obtained from a DC voltage that is equal to 1320 V. Figure 10(b) is a zoom in the output voltage. THD result of the FFT analyze will be presented in the section of Simulation and results.
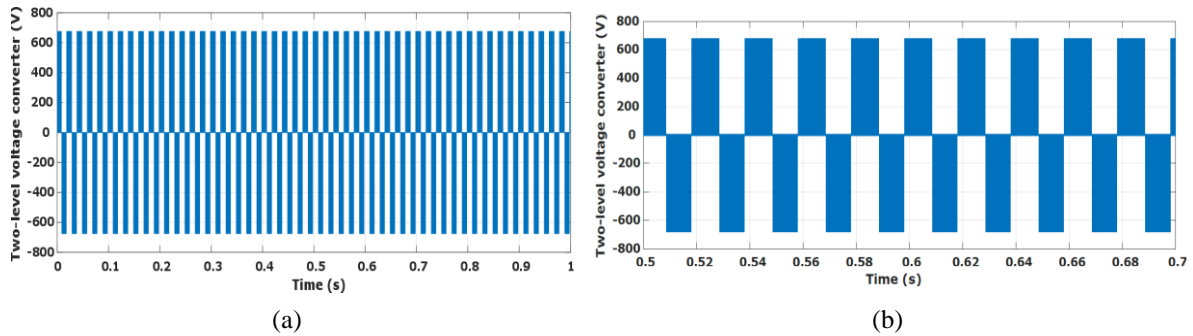

(a)

(b)

Figure 10. Simulation results of two-level inverter, (a) Output voltage and (b) Zoom in the output voltage

3.5. Model of the three-level inverter

The configuration of the NPC three-level inverter is presented in the Figure 11, it is composed two capacitor that divide the Vdc input voltage in order to converter it into a three level AC output voltage and three arms each one is composed of four IGBT switches, two diodes as presented in [25]. Switching sequences for the three-level inverter are generated through PWM controlled by a control system presented in the next section.
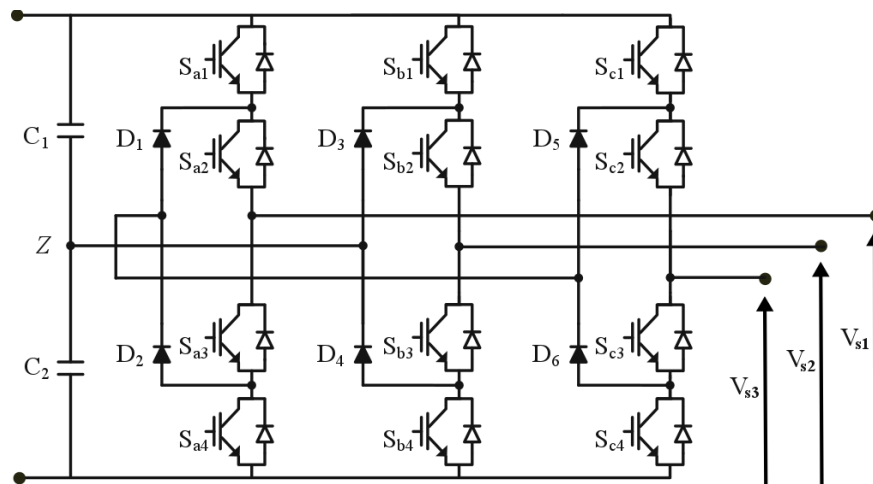

Figure 11. Configuration of three levels inverter

The three-level inverter function matrix is:

$$\begin{bmatrix} V_{s1} \\ V_{s2} \\ V_{s3} \end{bmatrix} = \frac{2}{3} U_{c1} \begin{bmatrix} 1 & -1 & -1 \\ -1 & 1 & -1 \\ -1 & -1 & 1 \end{bmatrix} \begin{bmatrix} S_{a1} \\ S_{b1} \\ S_{c1} \end{bmatrix} + \frac{2}{3} U_{c2} \begin{bmatrix} 1 & -1 & -1 \\ -1 & 1 & -1 \\ -1 & -1 & 1 \end{bmatrix} \begin{bmatrix} S_{a2} \\ S_{b2} \\ S_{c2} \end{bmatrix} \qquad (20)$$

Si are the Switching sequences applied by the PWM. In MATLAB/ Simulink we modeled and simulated the Three level inverter in order to observe the output waveform and analyze the THD before using it with WECS. Figure 12(a) present a single phase three level output voltage obtained from a DC voltage. Figure 12(b) presents a zoom in the results. THD result of the FFT analyze will be presented in the section of simulation and results.
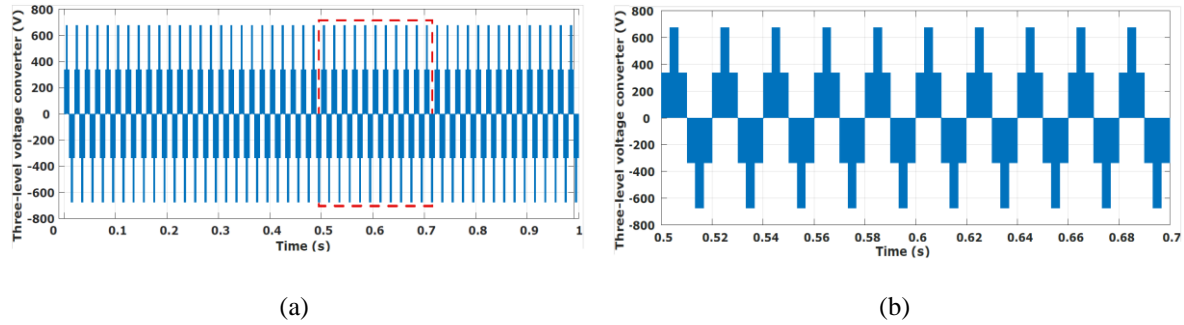
(a)	(b)

Figure 12. Simulation results of three-level inverter, (a) Output voltage and (b) Zoom in the output voltage

3.6. Model of the five-level multilevel inverter

The five-level inverter used is an H-Bridge structure cascaded composed of three arms in cascaded each one is composed of two capacitors that divide the input Vdc in two and two H-bridge inverter each one of them has 4 IGBT. The model of a three-phases five level cascade H-Bridge inverter is presented in Figure 13 and also developed in [19]–[26] and the switching sequences of switches is presented in Table 2 .
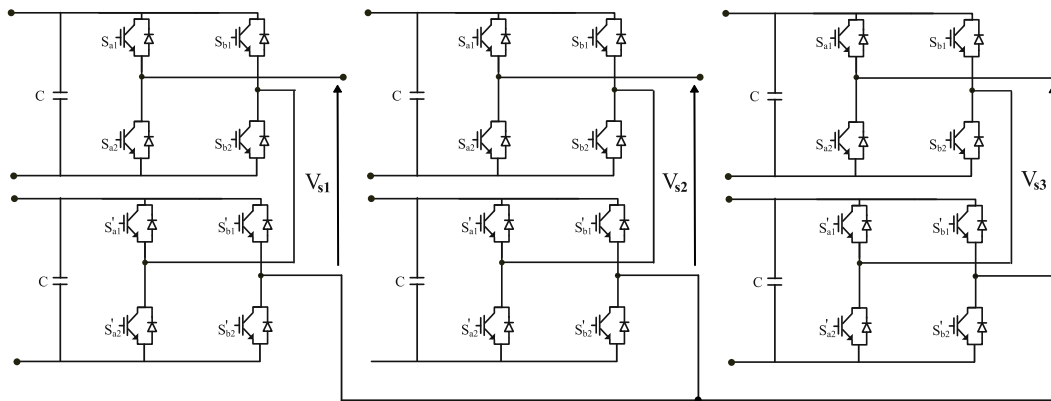
Figure 13. Model of three-phase five-level cascade H-bridge

Table 2. Switching state

S_1	S_2	S_2	S_4	S_1'	S_2'	S_3'	S_4'	V_{out}
1	1	0	0	0	0	1	1	0
1	0	0	1	1	0	0	1	0
1	0	0	1	0	1	1	0	0
0	1	1	0	1	0	0	1	0
0	1	1	0	0	1	1	0	0
0	0	1	1	1	1	0	0	0
1	1	0	0	1	0	0	1	V_{dc}
1	1	0	0	0	1	1	0	V_{dc}
1	0	0	1	1	1	0	0	V_{dc}
0	1	1	0	1	1	0	0	V_{dc}
1	1	0	0	1	1	0	0	$2V_{dc}$
0	0	1	1	1	0	0	1	$-V_{dc}$
0	0	1	1	0	1	1	0	$-V_{dc}$
1	0	0	1	0	0	1	1	$-V_{dc}$
0	1	1	0	0	0	1	1	$-V_{dc}$
0	0	1	1	0	0	1	1	$-2V_{dc}$

In MATLAB/Simulink we modeled and simulated the five-level inverter in order to observe the output waveform and analyze the THD before using it with WECS. Figure 14(a) presents a single phase five level output voltage obtained from a DC voltage. Figure 14(b) gives a zoom for this result. THD result of the FFT analyze will be presented in the section of simulation and results.
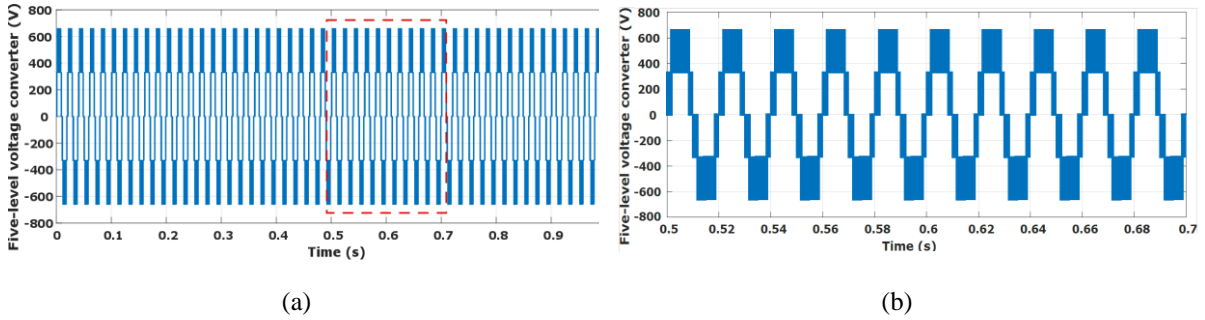
(a)   (b)

Figure 14. Simulation results of five-level inverter, (a) Output voltage and (b) Zoom in the output voltage

4.   WECS CONTROL STRATEGIE OF ACTIVE AND REACTIVE POWER

In this section, we present the control strategies used in our WECS in order to improve the quality of produced electrical energy for a better integration into the electrical grid. The global scheme of WECS and controllers is presented in the Figure 15.
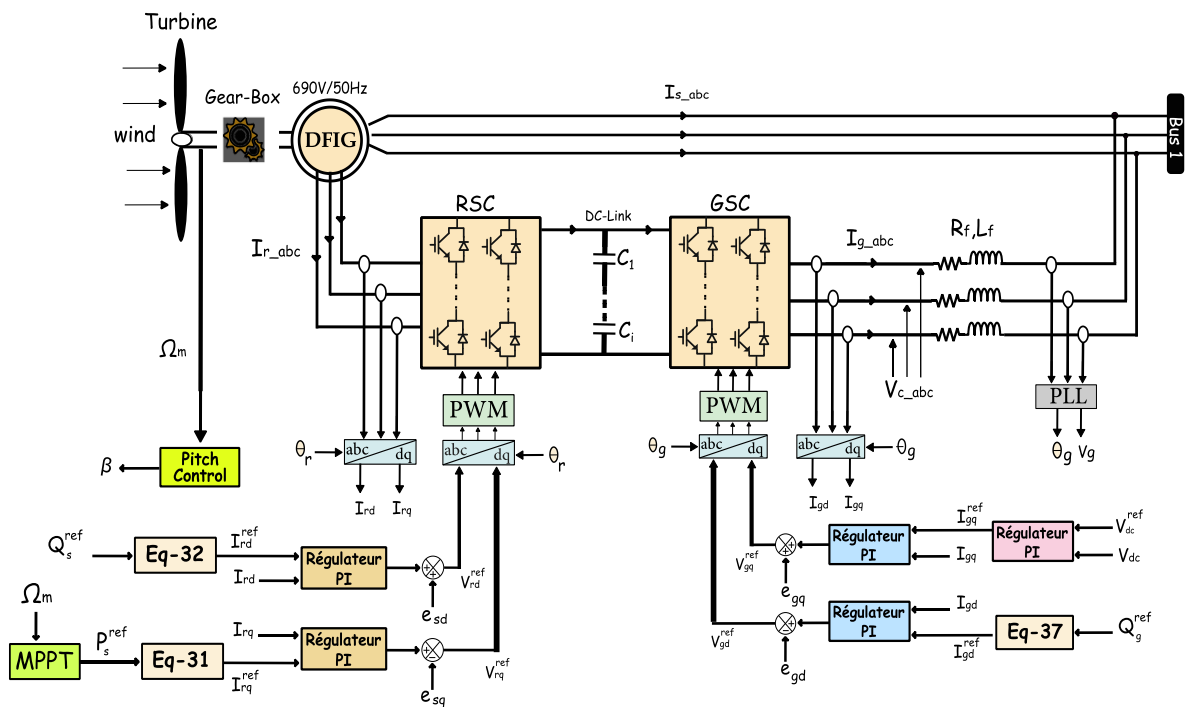

Figure 15. Control scheme of WECS

4.1. Maximum power point tracking algorithm

In order to extract maximum power possible from the kinetic energy of wind, a maximum power point tracking algorithm has been developed. For our WECS we used MPPT controller in order to track a specific speed for extracting maximum power from the wind despite the wind speed variation. The principle of this controller is to keep the tip speed ratio equal to an optimum value in order to maximize the power coefficient ($\lambda = \lambda^{opt}$; $C_p = C_p^{max}$). The maximum aerodynamic power can be expressed as,

$$P_{aero}^{max} = \frac{1}{2}\ \rho\ A_t\ \frac{C_p^{max}}{\lambda^{opt^3}}\ \frac{R^3}{G^3}\ \omega_{mec}^3 = K_{p_{opt}}\ \omega_{mec}{}^3 \tag{21}$$

$K_{p_{opt}}$ is optimal power coefficient.

$$K_{p_{opt}} = A_{wt}\ \frac{\rho}{2}\ \frac{C_p^{max}}{\lambda^{opt^3}}\ \frac{R^3}{G^3} \tag{22}$$

4.2. Pitch angle control

Other way for extracting maximum power is managing the orientation of blade by regulating the pitch angle β of blades. The blade orientation system consists on positioning the blades at a reference β^{ref} angle which depends on the direction of wind, this rotation is done by a servo motor. This system enables turbine blades to rotate using the Pitch control [27], [28]. The pitch angle β^{ref} depends upon the mechanical power control P_t. Pitch Angle β equation can be expressed as,

$$\beta = \frac{1}{1+T_\beta s} \beta^{ref} \tag{23}$$

s is a Laplace Operator; T_β is the constant time of the pitch servo.

4.3. Control strategy of the rotor-side inverter

For a better integration of the generated power into the grid a control of the used inverters is necessary, so in order to control the rotor-side inverter, we used the Indirect Stator Field Oriented Control (ISFOC), the principle of this control is orienting the stator field vector Ψ_s along the axis d [29]. So that: $\Psi_{sq} = 0$; $\Psi_{sd} = \Psi_s$. As known, in high and medium power machines the stator resistance R_s can be considered as negligible, and considering that the grid is stable, so that the stator field Ψ_s is constant.

DFIG model can be expressed as,

$$\frac{d}{dt}\begin{bmatrix} i_{rd} \\ i_{rq} \end{bmatrix} = \begin{bmatrix} -k_1 & \omega_r \\ -\omega_r & -k_1 \end{bmatrix}\begin{bmatrix} i_{rd} \\ i_{rq} \end{bmatrix} - \begin{bmatrix} 0 & -\omega_r k_3 \\ \omega_r k_3 & 0 \end{bmatrix}\begin{bmatrix} \Psi_s \\ 0 \end{bmatrix} + \begin{bmatrix} k_2 & 0 \\ 0 & k_2 \end{bmatrix}\begin{bmatrix} v_{rd} \\ v_{rq} \end{bmatrix} \tag{24}$$

et:

$$\begin{bmatrix} v_{sd} \\ v_{sq} \end{bmatrix} = \begin{bmatrix} 0 & 0 \\ \omega_g & 0 \end{bmatrix}\begin{bmatrix} \Psi_s \\ 0 \end{bmatrix} \tag{25}$$

$k_1 = \frac{R_r}{\sigma L_r}$; $k_2 = \frac{1}{\sigma L_r}$; $k_3 = \frac{Lm}{\sigma L_s L_r}$; $\omega_r = \omega_g - p\Omega_{mec}$.

The rotor angle expression is,

$$\theta_r = \int \left(\omega_g - \omega_{mec}\right) dt \tag{26}$$

As we are using the ISFOC, the compensation and the coupling terms could be expressed as,

$$\begin{bmatrix} e_{rd} \\ e_{rq} \end{bmatrix} = \frac{1}{k_2}\begin{bmatrix} 0 & \omega_r \\ \omega_r & 0 \end{bmatrix}\begin{bmatrix} i_{rd} \\ i_{rq} \end{bmatrix} + \frac{k_3}{k_2}\begin{bmatrix} 0 & 0 \\ \omega_r & 0 \end{bmatrix}\begin{bmatrix} \Psi_s \\ 0 \end{bmatrix} \tag{27}$$

Electromagnetic torque equation is,

$$T_{em} = -\frac{3}{2}\frac{pL_m}{L_s}\Psi_s i_{rq} \tag{28}$$

Active and reactive powers are,

$$P_s = -\frac{3}{2}\frac{L_m}{L_s}v_g i_{rq} \tag{29}$$

$$Q_s = \frac{3}{2}\left(-\frac{L_m}{L_s}v_g i_{rd} + \frac{\Psi_s}{L_s}v_g\right) \tag{30}$$

From the previous equations, we obtain the reference currents i_{rq}^{ref} and i_{rd}^{ref} for regulating the produced active and reactive power of the DFIG.

$$i_{rq}^{ref} = -\frac{2}{3}\frac{L_s}{p\Psi_s L_m}P_{aero}^{opt} \tag{31}$$

$$i_{rd}^{ref} = \frac{2}{3}\left(\frac{\Psi_s}{L_m} - \frac{L_s}{v_g L_m}Q_s^{ref}\right) \tag{32}$$

4.4. Control strategy of the grid-side inverter

In order to control the grid side inverter, we used the voltage-oriented control (VOC) because and according to [30], [31] it is considered one of the efficient controller for the grid side thanks to its lower energy losses and current distortion. The VOC used a Vdc control loop and an inner current control loop in order to have a fast dynamic response, so, $v_{gd} = 0$ and $v_{gq} = v_g$. The equations of P_f and Q_f are,

$$P_f = \frac{3}{2} v_g i_{fq} \tag{33}$$

$$Q_f = \frac{3}{2} v_g i_{fd} \tag{34}$$

The filter currents are:

$$\frac{\mathrm{d}}{\mathrm{d}t}\begin{bmatrix} i_{gd} \\ i_{gq} \end{bmatrix} = \begin{bmatrix} -k_4 & \omega_g \\ -\omega_g & -k_4 \end{bmatrix}\begin{bmatrix} i_{gd} \\ i_{gq} \end{bmatrix} + \begin{bmatrix} k_5 & 0 \\ 0 & k_5 \end{bmatrix}\begin{bmatrix} v_{id} \\ v_{iq} \end{bmatrix} + \begin{bmatrix} 0 & 0 \\ 0 & -k_5 \end{bmatrix}\begin{bmatrix} 0 \\ v_g \end{bmatrix} \tag{35}$$

$$k_4 = \frac{R_f}{L_f}; \ k_5 = \frac{1}{L_f}.$$

Using VOC we obtain a compensation and the coupling that are expressed as:

$$\begin{bmatrix} e_{gd} \\ e_{gq} \end{bmatrix} = \frac{\omega_g}{k_5}\begin{bmatrix} 0 & -1 \\ 1 & 0 \end{bmatrix}\begin{bmatrix} i_{gd} \\ i_{gq} \end{bmatrix} + \begin{bmatrix} 0 & 0 \\ 1 & 0 \end{bmatrix}\begin{bmatrix} 0 \\ v_g \end{bmatrix} \tag{36}$$

Direct reference current i_{fd}^{ref} is:

$$i_{fd}^{ref} = \frac{2}{3v_g} Q_f^{ref} \tag{37}$$

For this WECS, we are using a PI controller for a separate control of the injected electromechanical torque and flux of the DFIG. PI controller is also used in order to ensure a follow of reactive and active powers of the DFIG to their references. In Figure 16 we present the block diagram of the closed loop for the PI control strategy. The general PI controller expression is:

$$C(s) = K_p + \frac{K_i}{s} \ ; \ I_r(s) = \frac{k_r}{1+\gamma_r s} \ ; \ V(s) = \frac{1}{C s} \ ; \ I_f(s) = \frac{k_f}{1+\gamma_f s} \tag{38}$$

$$k_r = \frac{1}{R_r}, k_f = \frac{1}{R_f}; \gamma_r = \frac{\sigma L_r}{R_r}, \gamma_f = \frac{L_f}{R_f}.$$
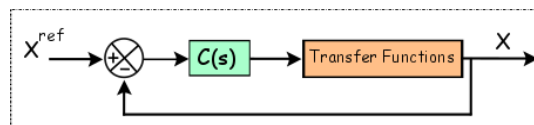

Figure 16. PI Controller loop

5. SIMULATION RESULTS AND DISCUSSION

For evaluating and testing the performance of our WECS, equipped with a pitch controller, an MPPT control strategy, and two multilevel inverters connected to the rotor and to the grid and controlled by an ISFOC for the rotor side and a VOC in the grid side as shown in Figure 15. We carried out multiple simulations in MATLAB/Simulink environment to verify the performances of each multilevel separately, using a variable wind speed profile, which varies between 8m/s and 12m/s as shown in Figure 17. The studied WECS, DFIG and grid parameters are listed in Tables 1, 2 and 3. Depending on the result of the WECS simulation presented in Figures 18(a) and Figure 18(b), we can conclude that our system has two functioning mode the first one is the MPPT used for wind speed that is less than 12 m/s. So, when the wind speed exceeds the nominal speed, the aerodynamique power is limited using the pitch control regulation and so that the power coefficient and tip speed ratio decreases.
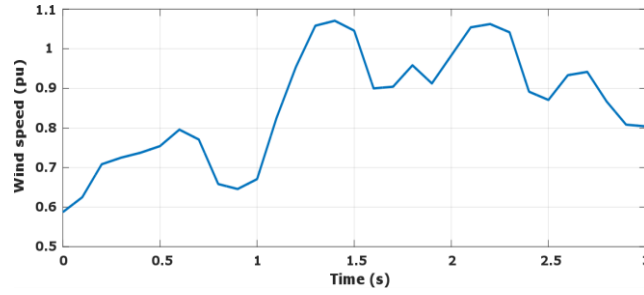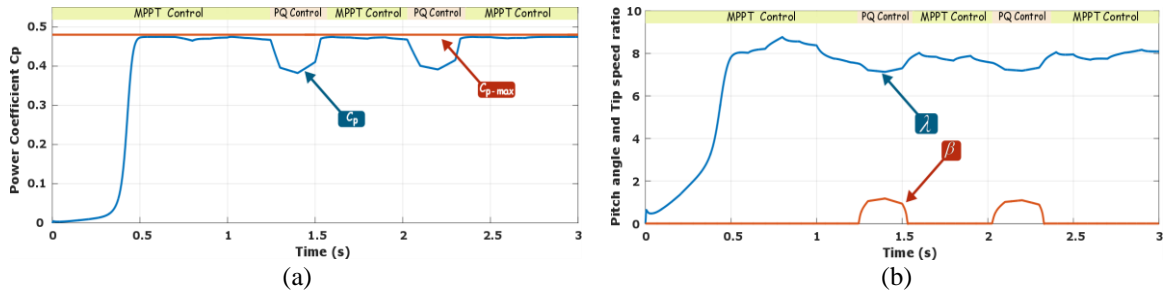
Figure 17. Wind speed profile

(a)

(b)

Figure 18. Simulation results of power coefficient and it's parameters, (a) Power coefficient and (b) Speed ratio and pitch angle

Figure 19(a) show that active power follows its reference as explained theoretically in the previous section. Figure 19(b) shows the same things for reactive power. Figure 20 present the output voltage Vdc of the rotor side inverter this result shows that it's equal to its reference V_{dc_ref} = 1000 V. We also presented the injected grid voltage in blue and stator current in orange in the Figure 21, the current and voltage are not in phase and as we conclude, at the start-up time the current is equal to zero and then start to increase and varies depending on the wind profile

(a)

(b)
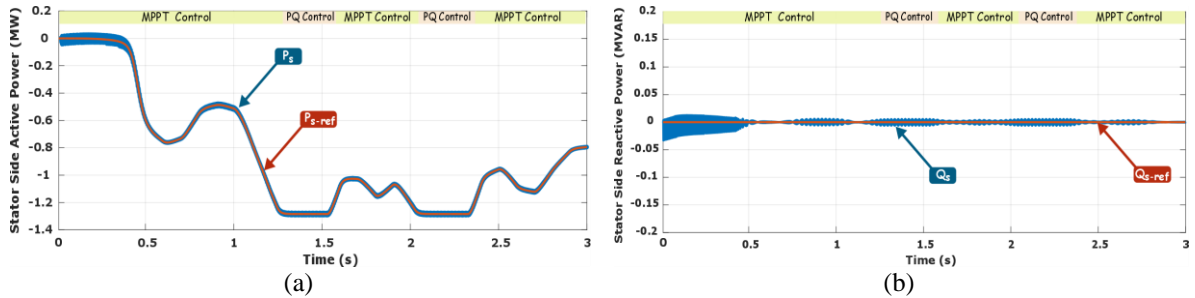
Figure 19. Simulation results of active and reactive power of the DFIG: (a) active power and (b) reactive power
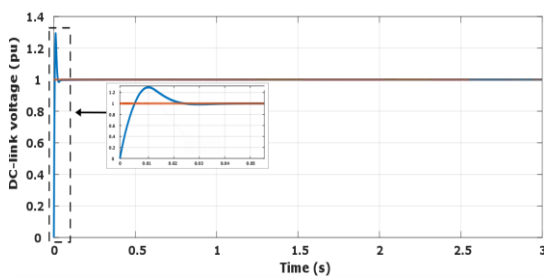
Figure 20. Vdc voltage
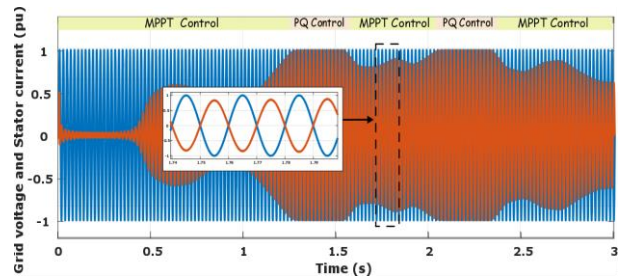
Figure 21. Grid voltage and stator current

        This first part of simulation was only dedicated for the control of active and reactive powers of our WECS based on DFIG, a 5 level cascaded H-bridge multilevel inverter and a VOC and ISFOC controllers using a PI controller. The main objective of these controls is to extract the maximum power possible from the available wind speed in order to inject it safely into the grid. The obtained resulted of simulation by MATLAB/SIMULINK proved the efficacy of those controls strategies of regulating the active and reactive powers of our WECS. In this part we are going to highlights the performance of the 3 proposed multilevel inverter topologies studied in section 3 used for our WECS and that's by elaborating a comparative study of the THD factor resulted from an FFT analyze done for the current that will be injected to the grid i_g , the stator current is and the filter output current if . In Figure 22(a) we present the THD result using a two level inverter of the currents if, is in Figure 22(b) and i_g in Figure 22(c).
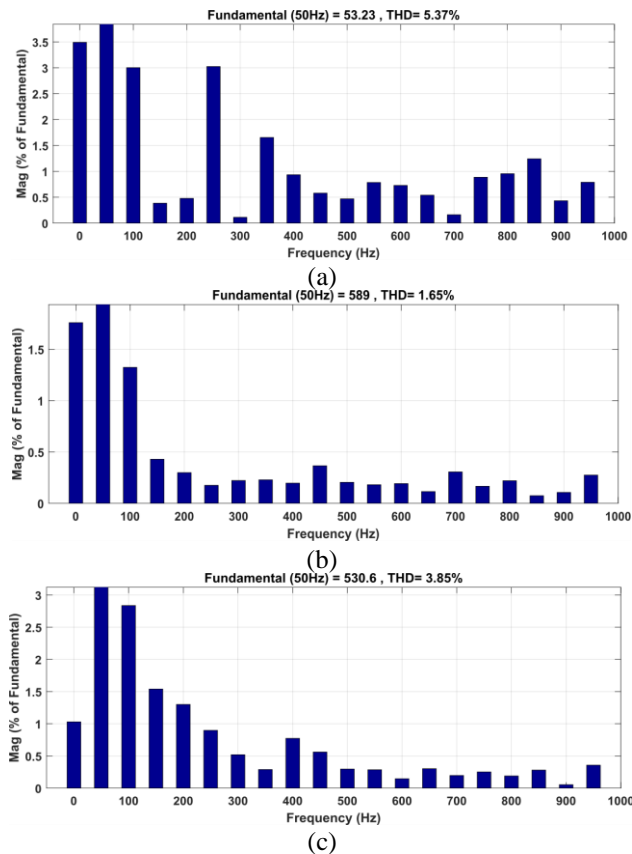

Figure 22. FFT analyze result of currents of WECS using two-level inverter, (a) i_f current, (b) i_s current, and (c) i_g current

        Figures 23(a), 23(b), and 23(c) presents the THD of if, is and i_g using the three level inverter studied in section 3, and as we can see the THD factor has been reduced by 1.62% for current if, 0.67% for current is and 0.41% for current i_g in comparison with the two level one. Figure 24(a), 24(b) and 24(c) presents the THD of if, is and i_g using the cascaded H-bridge 5 level inverter studied in section 3, and as we can see the THD factor has been reduced by 0.02% for current if, 0.49% for current is and 2.59% for current i_g in comparison with the three level one and by 1.65% or current if, 1.16% for current is and 3% for current i_g in comparison with the result of the two-level inverter. We can conclude that the use of multilevel inverter in addition to the amelioration of the output voltage form studied in section 3 it decreased significantly the THD factor of the current that will be injected to the grid which is less than 5% and makes our WECS satisfy the IEEE 519 standards. Table 3 resumes THD results.

Table3. THD results conclusion

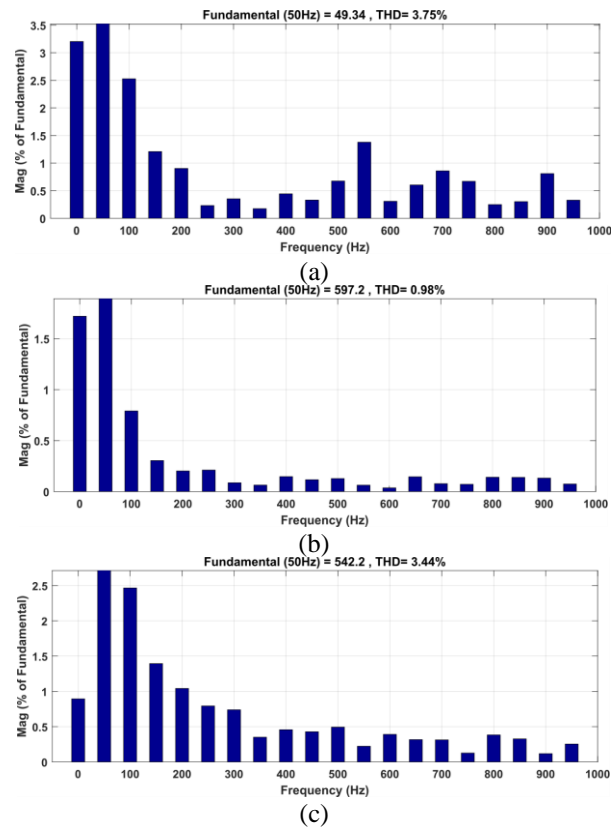| THD	I_f (%)	I_s (%)	I_g (%)
2 level	5.37	1.65	3.85
3 level	3.75	0.98	3.44
5 level	3.72	0.49	0.85

(a)

(b)

(c)

Figure 23. FFT analyze result of currents of WECS using three-level inverter, (a) i_f, (b) i_s, and (c) i_g
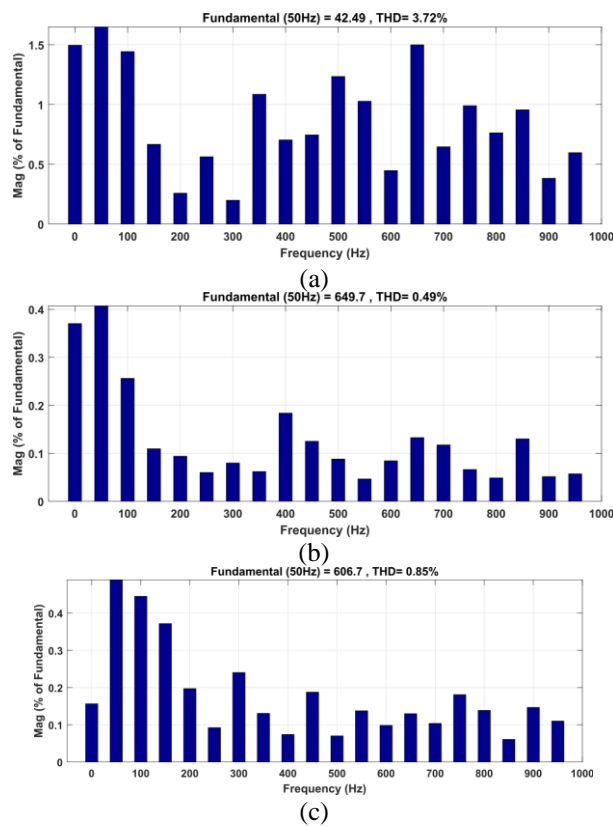

(a)

(b)

(c)

Figure 24. FFT analyze result of currents of WECS using 5 level inverter: (a) i_f, (b) i_s, and (c) i_g.

6.   CONCLUSION

This paper presents a comparative analyze and study of the performances of using multilevel inverter for WECS application. The theoretical study has been confirmed by an FFT analyze simulation done in MATLAB/Simulink which proved that THD factor of the current that will be injected to the grid have been reduced significantly using a 5 level inverter instead of three and two level ones. Moreover, the use of multilevel inverter for WECS instead of the conventional one present more advantages as a smoother output waveform which enable us to minimize the size of the filter or even eliminating it for higher levels also the dv/dt stress and EMI are reduced so that the dimensions of semiconductors used and consequently the cost of the inverter. By this theoretical and simulation results we aim to compare it with a practical one in order to confirm our study.

REFERENCES

[1]   Statistical Review report of World Energy, 70th edition, Centre for Energy Economics Research and Policy, Heriot-Watt University 2021.
[2]   Global Energy Trends 2021 edition - Enerdata.
[3]   R.Mukand Patel. Wind and solar power systems, Chapter 2 "Wind Power" CRC Press, U.S. Merchant Marine Academy Kings Point, New York. 1999.
[4]   Muhammad H. Rashid, Chapter 8 Multilevel inverter of "Power Electronics, circuit, devices, and application"Third Edition University of Florida. pp.253-255.2009.
[5]   A. Nabae, I. Takahashi, and H. Akagi. "A New Neutral-Point-Clamped PWM inverter" *IEEE Transactions on Industry Applications*, pp. 518–523, 1981, doi: 10.1109/TIA.1981.4503992.
[6]   J. Rodriguez, J. S. Lai, and F. Z. Peng, "Multilevel Inverters: A Survey of topologies ,controls and applications" *IEEE Transaction on industrial Electron*, voI .49, no. 4, pp. 724–738, August 2002, doi: 10.1109/TIE.2002.801052.
[7]   E. Elnady and A. Adam, "Multilevel inverter operated by voltage rientation control" 2016 5th International Conference on Electronic Devices, Systems and Applications (ICEDSA), 2016, pp. 1–4, doi: 10.1109/ICEDSA.2016.7818466.
[8]   S. Elaimani, " Modelisation of diffrent topologies of Wind system integrated in the electrical grid", *thesis report, L2EP of Lille,* 2004.
[9]   B.Benyacho; F.Ait Ouhrouch; K.Gueraoui. " Modelisation in MATLAB/ SIMULINK of a wind turbine related to a DFIG". *13th Edition of Meknes*, 2017.
[10]   P.Krafczyk . "Modelisation and implementation of a production Wind system using a DFIG", thesis report, Lorrraine university, 2013.
[11]   S. Muller, M. Deicke, and R. W. De Doncker, "Doubly-fed induction generators systems for wind turbines" *IEEE Industry Applications Magazine*, vol. 3, no. 3, pp. 26–33, 2009, doi: 10.1109/2943.999610.
[12]   H. Overdeth, T. M. Undeland, and T. Gjengedal, "Doubly Fed Induction Generator in a Wind Turbuine" *Wind Power and the impacs on Power Systems,* IEEE Workshop, Oslo,2002.
[13]   M. Nadour, A. Essadki, T. Nasser, and M. Fdaili, "Robust coordinated control using backstepping of flywheel energy storage system and DFIG for power smoothing in wind power plants" *International Journal of Power Electronic and Drove Systems*, vol. 10, no. 2, pp. 1110–1122, June 2019, doi: 10.11591/ijpeds.v10.i2.pp1110-1122.
[14]   H. Laghridat, A .Essadki, M. Annoukoubi, and T. Nasser, "A Novel Adaptive Active Disturbance Rejection Control Strategy to Improve the Stability and Robustness for a Wind Turbine Using a Doubly Fed Induction Generator" *Journal of Electrical and Computer Engineering,* vol. 2020, pp 1–14, 202, doi: 10.1155/2020/9847628.
[15]   J. Rodr´ıguez, J-S. Lai, and F. Z. Peng, "Multilevel inverters: a survey of topologies, controls, and applications" *IEEE Transactions on Industrial Electronics*, vol. 49, no. 4, pp.724–738, Aug. 2002, doi: 10.1109/TIE.2002.801052.
[16]   K. K. Gupta and S. Jain, "Topology for multilevel inverters to attain maximum number of levels from given DC sources" *IET Power Electronics*, vol. 5, no. 4, pp. 435–446, April 2012, doi: 10.1049/iet-pel.2011.0178.
[17]   H. Abu-Rub, M. Malinowski, and K. Al-Haddad, "Multilevel Converter/Inverter Topologies and Applications" in *Power Electronics for Renewable Energy Systems, Transportation and Industrial Applications*, 1ˢᵗ Ed, Willwy-IEEE Press, pp. 422–462, 2014.
[18]   L. Zhang , S. Watkins, and W. Shepherd, "Analysis and control of a multi-level flying capacitor inverter" *IEEE International Power Electronics Congress*, 2002, pp. 66–71, doi: 10.1109/CIEP.2002.1216638.
[19]   M. Annoukoubi, A. Essadki, and T. Nasser, "Cascade H-Bridge Multilevel Inverter for a Wind Energy Conversion System Applications" *2021 9th International Renewable and Sustainable Energy Conference (IRSEC)*, 2021, pp. 1–7, doi: 10.1109/IRSEC53969.2021.9741171.
[20]   K. A. Corzine, M. W. Wielebski, F. l. Peng, and J. Wang, "Control of cascaded multilevel inverters" *IEEE Transaction on Power Electronics*, vol. l9, no. 3, pp. 732–738, May 2004, doi: 10.1109/TPEL.2004.826495.
[21]   W.Hiber."Harmonic Analysis in an elctrical grid with a Wind energy production ", *Thesis report, Algeria*, 2013.
[22]   P. Palanivel and S. S. Dash, "Analysis of THD and output voltage performance for CMU using carrier pulse width modulation techniques" *lET Power Electronics*, vol. 4, no. 8, 2011, doi: 10.1049/iet-pel.2010.0332.
[23]   P. Delarue, P. Bartholomeus, F. Minne, and E. Dejaeger, "Study of harmonic currents introduced by three-phase PWM-converters connected to the grid" *17th International Conference on Electricity Distribution*, pp. 1–6, 2003.
[24]   S. Elaimani, B. Francois, B. Robyns, and F. Minnie, "Modelling of generated harmonics from a wind energy conversion system based on a doubly fed induction generator," *Electromotions*, vol. 10, no. 4, pp. 1–6, 2003.
[25]   M. Annoukoubi, A.Essadki, H. Laghridat, and T. Nasser, "Comparative study between the performances of a three-level and two-level converter for a Wind Energy Conversion System" 2019 International Conference on Wireless Technologies, Embedded and Intelligent Systems (WITS), 2019, pp. 1–6, doi: 10.1109/WITS.2019.8723739.
[26]   J. Patel, R. Kapadia, and D. Patel, "Simulation and Analysis of Cascaded H Bridge Multilevel Inverter using Single DC source" *International Journal of Emerging Technology and Advanced Engineering*, vol. 3, no. 8, pp. 633–637, April 2013, doi: 10.1.1.413.4009.

[27] I. Aboudrar, S. El Hani, H. Mediouni, and A. Aghmadi, "Modeling and robust control of a grid connected direct driven PMSG wind turbine by ADRC" *Advances in Electrical and Electronic Engineering*, vol. 16, no. 4, pp. 402–413, 2018, doi: 10.15598/aeee.v16i4.2952.

[28] H. Laghridat, A. Essadki, and T. Nasser, "Comparative analysis between PI and linear-ADRC control of a grid connected variable speed wind energy conversion system based on a squirrel cage induction generator" *Mathematical Problems in Engineering*, vol. 2019, pp. 1–16, 2019, doi: 10.1155/2019/8527183.

[29] H. Jingqing. "From PID to active disturbance rejection control" *IEEE transactions on Industrial Electronics*, vol. 56, no. 3, p. 900–906, 2009, doi: 10.1109/TIE.2008.2011621.

[30] B. Robyns, Y. Pankow, L. Leclerq, and B. François, "Equivalent continuous dynamic model of renewable energy systems" *7th International Conference on Modeling and Simulation of Electric Machines, Converters and Systems: Electrimacs*, 2002, pp. 1.

[31] C. Hamid, A. Derouich, T. Hallabi, O. Zamzoum, M. Taoussi, S. Rhaili, and O. Boulkhrachef, "Performance improvement of the variable speed wind turbine driving a DFIG using nonlinear control strategies" *International Journal of Power Electronics and Drive Systems*, vol. 12, no. 4, pp. 2470–2482, Dec. 2021, doi:10.11591/ijpeds.v12.i4.pp2470-2482.

BIOGRAPHIES OF AUTHORS

Maha Annoukoubi ⓘ 🄶 SC ⓟ is an electrical engineer and PHD student in electrical engineering in the Research Centre of Engineering and Health Sciences and Technologies (STIS) of the National School of Arts and Crafts in Rabat (ENSAM), Mohammed V University, Morocco, since 2018. Her research interests are related to renewable energy and power systems. Her current activities are the impact of using multilevel inverter for WECS. She can be contacted at email: m.annoukoubi@gmail.com.

Ahmed Essadki ⓘ 🄶 SC ⓟ is a research professor in the Research Centre of Engineering and Health Sciences and Technologies (STIS). And a professor of the electrical engineering at National School of Arts and Crafts in Rabat (ENSAM), Mohammed V University, Morocco. In 2000, He received his PhD degree from Mohammadia Engineering School (EMI), (Morocco). From 1990 to 1993, he pursued his Master program at UQTR University, Quebec Canada, respectively, all in electrical engineering. His current research interests include renewable energy, motors drives and power system. He can be contacted at email: ahmed.essadki.ensam@gmail.com.

Hammadi Laghridat ⓘ 🄶 SC ⓟ received the M. S degree in electrical engineering in 2016 from Mohammed V University, ENSET Rabat-Morocco. Currently he is working toward the Ph.D. in the Research Centre of Engineering and Health Sciences and Technologies (STIS), since 2017. His research interests are related to renewable energy. His current activities include advanced supervision and controls strategies of a wind farms for ancillary services. He can be contacted at email: hammadi.laghridat@um5s.net.ma.

Tamou Nasser ⓘ 🄶 SC ⓟ is currently an Associate Professor at the communication networks department of National High School for Computer Science and Systems (ENSIAS), Mohammed V University, Morocco, since 2009. She received her PhD degree in 2005 and her research MS degree, in 2000, respectively, all in electrical engineering from Mohammadia Engineering School (EMI), Morocco. Her research interest's renewable energy, motor drives, power system, and Smart Grid. She can be contacted at email: tamounasser@gmail.com.